Molecular Science

AIMS Molecular Science, 9(4): 136–144.
DOI: 10.3934/molsci.2022008
Received: 27 September 2022
Revised: 17 November 2022
Accepted: 22 November 2022
Published: 05 December 2022

http://www.aimspress.com/journal/Molecular

Research article

High-yield production and purification of the fusion pH-responsive peptide GST-pHLIP in *Escherichia coli* BL21

Oscar Cienfuegos-Jiménez[1], Abril Morales-Hernández[1], Olivia A. Robles-Rodríguez[1], Sergio Bustos-Montes[1], Kevin A. Bañuelos-Alduncin[1], Aurora R. Cortés-Castillo[1], Hugo D. Barreto-Hurtado[1], Luis Carrete-Salgado[1] and Iván A. Marino-Martínez[1,2,*]

[1] Unidad de Terapias Experimentales, Universidad Autónoma de Nuevo León, Centro de Investigación y Desarrollo en Ciencias de la Salud (CIDICS), Monterrey, Nuevo León, México
[2] Departamento de Patología, Universidad Autónoma de Nuevo León, Facultad de Medicina, Monterrey, Nuevo León, Mexico

* **Correspondence:** Email: amarinomtz@gmail.com.

Abstract: The pH Low Insertion Peptide (pHLIP) has versatile applications in several diseases due to its differential behavior at slightly different pH values. pHLIP is an unstructured and peripheral membrane-associated peptide at neutral pH and an α-helical transmembrane peptide at acidic values. Similar to what happened to insulin and growth hormone, pHLIP´s expanding applications require high-yield production to further scale-up its usefulness. To date, synthesis of the pHLIP has not been reported in a prokaryotic platform, mainly relying on solid-phase synthesis. Bacterial production arises as an option for high-amount peptide generation and larger pHLIP fusion protein-synthesis; however, cell-based pH-responsive peptide production could be challenging due to intracellular peptide interactions or degradation due to unstructured conformations. An *Escherichia coli* (E. coli)-BL21 cell culture was induced with Isopropyl ß-D-1-thiogalactopyranoside (IPTG) in order to produce a Glutathione S-transferase-pHLIP (GST-pHLIP) fusion construct. Purification was done with Glutathione (GSH)-decorated magnetic beads using 4 ml of the induced cell culture. The production was quantified with Bradford reagent and characterized with SDS-PAGE and Western blot, contrasting Bradford results with densitometry analysis to obtain production approximate absolute values. A purified approximate total yield of ~26 µg with an apparent GSH-bead saturation and a total production of ~82 µg was obtained. Our Western Blot assay confirmed the presence of the GST-pHLIP construct in all the IPTG-induced fractions. Conclusion: A high-yield pHLIP production irrespective of its membrane affinity in acidic

environments or its unstructured nature was achieved. Our study could be useful to scale up pHLIP synthesis for future applications.

Keywords: pH Low Insertion Peptide; pHLIP; membrane protein; Escherichia coli; protein production

Abbreviations: IPTG: Isopropyl ß-D-1-thiogalactopyranoside; ATRAM: acidity-triggered rational membrane; pHLIP: pH Low Insertion Peptide; E. coli: *Escherichia coli*; GST: Glutathione S-transferase; LB: Luria-Bertani broth; GSH: Glutathione; IP: IPTG-induced purified protein; NIP: IPTG non-induced purified protein; IFT: IPTG-induced purification flow through; NIFT: IPTG non-induced purification flow through; ICL: IPTG-induced crude lysate; UCL: Untransformed cell lysate

1. Introduction

Membrane partition pH-responsive peptides could be defined as short amino acid sequences capable of spanning cell membranes in an inducible manner in response to changes in pH. Since pH is a commonly deregulated parameter in several diseases [1], these molecules have acquired great attention due to their applications to spot these conditions at the subcellular level. Several peptides with these properties have been reported to date, including the acidity-triggered rational membrane (ATRAM) peptide [2] and the pH Low Insertion peptide (pHLIP) [3].

pHLIP is a 35 amino acid long peptide, originally obtained from the Bacteriorhodopsin C helix [4], that possesses a remarkable sensitivity to slight changes of pH. The pH responsiveness of the peptide is manifested in a structural and behavioral distinction between two different pH conditions. At near neutral values and in the presence of biological membranes, the peptide presents many unstructured microstates either in soluble or membrane-associated fashion. However, at acidic pH the peptide adopts a structured transmembrane α-helix that traverses a membrane bilayer in a directional manner, with the C-terminus facing the cytoplasm and the N-terminus facing the extracellular milieu [5].

Due to the aforementioned properties, the pHLIP technology is currently employed for biophysical studies [6], imaging/diagnosis [7] and therapy [8], among others. In the biophysical field, the peptide has demonstrated usefulness to study membrane protein folding [9], partition between different dielectric media [10], thermodynamics of α-helix secondary structures [6] and kinetics [11]. Furthermore, by labeling the peptide with fluorophores at its N terminus or adding polar molecules at its C-terminus, the pHLIP has been used to identify acidic regions like tumors [12] or inflammatory zones [13] or translocate otherwise impermeable drugs through the cell membrane to reach cytoplasmic targets, respectively [14].

Solid-phase synthesis of the peptide has been widely employed as the main methodology to obtain useful concentrations of the molecule [3]. This technique can be advantageous given the misfolded or unstructured nature of pHLIP in solution, which could presumably make it prone to degradation after ribosomal synthesis [15]. However, bacterial production could be an attractive alternative that can offer a cheaper, affordable and reproducible option, producing higher yields. Moreover, bacterial production is compatible with the incorporation of radioactive amino acids that can label the peptide for tracking or imaging purposes [16] and can bypass the challenges posed by the acidic environment of the eukaryotic biosynthetic pathway of newly synthesized proteins, which could complicate pH-responsive peptide

synthesis [17]. Given the peptide size, solid-phase synthesis is useful for production of the molecule at certain amounts; however, some applications can rely on pHLIP fusion proteins for peptide labeling, like the ones in immunotherapy [18], making chemical synthesis less practical as the protein length increases. Nonetheless, if antibody generation against the peptide is desired via immunization of animal models, a carrier protein must be ideally conjugated because of the size of the peptide [19], again augmenting its complexity for chemical synthesis. Therefore, due to the promising results of pHLIP, production of this and other pH-responsive protein agents are of great interest to further scale up the aforementioned applications to patients in the future, with the consequent necessity of large production capabilities.

In this study, high-yield production and purification of a pHLIP fusion protein in *Escherichia coli* (E. coli) BL21 are achieved; this is the first report of production of a pH-responsive peptide in a bacterial platform so far. With this report, we aim to demonstrate the conditions in which pH-responsive polypeptides could be efficiently generated, despite their affinity for biological membranes inside the producer cell or unstructured nature that otherwise could hamper efficient production and further purification.

2. Materials and methods

2.1. Cloning

The wt-pHLIP gene (which encodes the sequence AEQNPIYWARYADWLFTTPLLLLDLALLVDADEGT) was cloned in pGEX-4T1 between BamHI and NotI restriction sites, downstream and in frame with the Glutathione S-transferase (GST) gene, to obtain a GST-tagged pHLIP (GST-pHLIP) product to aid further purification. This vector contains an Ampicillin resistance gene as a selection marker in bacteria along with the LacZ operon to control the expression of the gene of interest.

2.2. Bacteria transformation

Calcium-competent E. coli BL21 cells were prepared and transformed with the pGEX-4T1-pHLIP vector via heat shock. The cells were seeded in Luria-Bertani Broth (LB) Ampicillin-added agar plates (50 μg/mL Ampicillin, 10 g/L tryptone, 5 g/L yeast extract, 10 g/L NaCl and 15 g/L agar) along with transformation controls and incubated overnight. After successful selection, an individual colony was picked and grown overnight in 5 mL LB Ampicillin-added liquid medium (50 μg/mL Ampicillin, 10 g/L tryptone, 5 g/L yeast extract and 10 g/L NaCl) as a pre-inoculum.

2.2.1. Isopropyl ß-D-1-thiogalactopyranoside (IPTG) induction

A volume of 100 μL of the pre-inoculum was used to inoculate 100 mL of Ampicillin-added LB liquid medium until 0.8 O.D. 600 nm was reached. Gene expression-induction was done overnight at room temperature with continuous agitation, administrating 200 μL of 100 mM IPTG directly on cell cultures (slow IPTG-induction). This procedure was done in parallel with a non-induced control.

2.2.2. Cell lysis and protein purification

4 mL of the previously mentioned cell cultures was pelleted. After discarding the supernatant,,the pellet was subjected to two brief freeze-thaw cycles between −20 °C and room temperature and then resuspended in 200 µL of MagneGST Lysis Buffer from the MagneGST™ Protein Purification System (Promega, Madison, WI, USA; Catalog No. V8600) following sonication with Fisherbrand™ Sonicator 505 (Fisher Scientific) using 10 short bursts of 10 seconds with 30 second intervals for cooling. Purification was performed with the MagneGST Protein Purification System kit using 25 µL of the settled magnetic beads for each purification, and the rest of the procedure was done following the manufacturer instructions. As previously mentioned, this kit contains magnetic Glutathione (GSH) decorated beads that can bind GST tagged proteins. The purification product was eluted in 200 µL of nuclease free water, purifications flow through were conserved for further analysis in a 250 µL elution, along with crude lysates that were resuspended in 200 µL nuclease free water.

2.3. Protein quantification (raw data)

Six different protein fractions were evaluated in triplicate in a Quick Start™ Bradford Protein Assay (Bio-Rad, Hercules, CA, USA; Catalog No. 5000204) using the iMark™ Microplate Absorbance Reader (Bio-Rad): a fraction corresponding to the IPTG-induced purified protein (IP), a second fraction corresponding to the IPTG non-induced purified protein (NIP), a third fraction containing the IPTG-induced purification flow through (IFT) that contains the not GSH-bound eluate, a fourth fraction containing the IPTG non-induced purification flow through (NIFT) that is reciprocal to the previous one, a fifth fraction corresponding to the IPTG-induced crude lysate (ICL) and a sixth fraction containing the crude lysate of an untransformed cell culture (UCL). The production was then evaluated with SDS-PAGE, qualitatively visualizing the aforementioned six fractions with Coomassie gel staining, using the Precision Plus Protein Dual Color Standards molecular weight marker (Bio-Rad, Hercules, CA, USA; Catalog No. 1610374), and complemented with densitometry analysis using the Molecular Imager® Gel Doc™ XR System device (Bio-Rad) and Image Lab 6.1 Software (Bio-Rad, Hercules, CA, USA).

In order to determine the production yield per single purification assay and whole bacteria production yield, a comparison of densitometry data per lane with Bradford quantification assay was done. Using the Image Lab Software, the densitometry lane percentage of the band corresponding to the protein of interest in each of the IPTG-induced fractions was determined. The lane percentage corresponds to the percentage of the adjusted total band volume with respect to the adjusted total lane volume. A correction was done, applying the aforementioned lane percentage to the values obtained in the Bradford assay to each fraction. These results were taken as the approximate absolute concentration values. Total yield was calculated by multiplying the approximate absolute concentrations obtained by the elution volume previously mentioned for each fraction.

2.4. Western blot

Western Blot was performed using a goat anti-GST IgG polyclonal primary antibody (Cytiva, Washington, DC, USA; Catalog No. 27457701v) and a rabbit anti-goat IgG, HRP conjugated polyclonal antibody (Sigma Aldrich, Burlington, MA , USA; Catalog No. AP106P), revealed with Clarity™

Western ECL Substrate (Bio-Rad, Hercules, CA, USA; Catalog No. 1705060) and visualized in a ChemiDoc™ XRS+ System (Bio-Rad).

3. Results and discussion

In our study, the calculated molecular weight of the fusion peptide is ~29 kDa. It is expected that the volume of settled magnetic beads employed in our protocol has a binding capacity of 125–250 μg of GST bound protein. Nevertheless, in our experiment, proteins purified from 4 ml of cell culture reached bead saturation at ~26 μg of total yield or 131.1 mg/L of approximate absolute concentration (Table 1). This could be due to the small size of our peptide (35 aa), since the expected binding capacity of the beads is calculated considering a mean size protein (~300 aa). However, the number of peptides bound to each bead should be at a maximum in our assay, since the lane of the purification flow through of the IP fraction evidenced a band corresponding to residual or unbound peptide that is eluted at the end of the purification step (Figure 1, panel A). Moreover, the approximate absolute concentration in the IFT fraction is approximately double the one found in the IP fraction (Table 1). This result means that a higher yield can be purified from the cell culture volume used in our study. As expected, a 29% lane percentage in the IP fraction, in contrast with 14% in the IFT fraction, was found, since the latter has all the proteins that do not bind to GSH. This 29% also represents the estimated purity of the fusion protein and could also explain the saturation of the beads with ~26 μg of total yield, since non-specific binding of other proteins apparently occur, as suggested by the densitometry analysis (Table 1) (Figure 1, panels B and C). Next, the concentration and approximate total yield of the whole production in E. coli BL21 were calculated. Our correction of the Bradford values indicated that a total yield of almost 82 μg was produced at a concentration of ~409 mg/L in the ICL fraction (Table 1) (Figure 1, panel D). This total value is approximately the sum of the IP and IFT fractions, as expected since both of these fractions come from the ICL fraction. No visible band of interest was found in the NIP, NIFT or UCL fraction (Figure 1, panel A).

Table 1. Results of protein quantification.

Fraction	Mean Bradford concentration (mg/L)	Adjusted Total Band Volume [a]	Adjusted Total Lane Volume [a]	Lane %	Approximate absolute concentration (mg/L)	Approximate Total Yield (μg)
IP	452.1	1417839	4872298.9	29.1	131.1	26.2
IFT	1698.1	1544772	11275708	13.7	237.7	59.4
ICL	3152.6	2342214	17479208.9	13.4	409.8	81.9

Note: [a] Dimensionless units.

In order to confirm the production of the pHLIP, a qualitative Western Blot was performed. The analysis revealed 3 intense bands corresponding to the IP, IFT and ICL fractions, as expected (Figure 2). No signal was detected in the rest of the fractions, confirming the presence of the GST-pHLIP fusion protein.

It is important to note that our study only determines the production of the pHLIP but does not characterize its functionality. Since its initial studies, the pHLIP has been synthesized by chemical methods (e.g., t-BOC chemistry) [20]. It could be argued that this is convenient due to the absence of

post-translational modifications that can be added to the peptide in biological platforms and that can ultimately hamper its membrane translocation functionality, given the fact that the behavior of the pHLIP mainly depends on a delicate equilibrium in the peptide to membrane distance or dehydration towards membrane approximation (Born effect) [21]. Nonetheless, amino acid pKa deviations from bulk solution exposure values, from which pH sensitivity arises, depend on electrostatic interactions, hydrogen bonding and exposure to poor dielectric media of titratable residues [22], factors that can be dramatically affected by adding molecules post-translationally to the peptide. However, given the bacterial nature of the peptide as the C helix of Bacteriorhodopsin and its transmembrane origin [20] which theoretically forbids any polar post-translational modification, it could be postulated that functional bacterial production is also feasible and even more convenient if scaling to higher yields is intended in the future or simply if its functional analysis after bacterial production is desired. Nevertheless, it remains to be addressed if synthesizing the C helix alone changes the dynamics of peptide biogenesis, since it is well known that multi-spanning membrane protein synthesis, like Bacteriorhodopsin, translocon passing and ultimately protein folding, depends on signal sequences, charge distribution and cooperativity with previously synthesized α-helices [23,24], with all of these factors absent in the individual pHLIP biosynthesis. This could ultimately prevent peptide accommodation in the membrane in the great majority of occasions, as previously suggested [25], exposing it to post-translational modifications. However, this possible outcome, if occurring, remains to be studied or confirmed. Finally, it is well known that unfolded proteins are actively degraded in cells [19]; however, we had no major complications in producing the peptide in E. coli BL21. This could be due to its GST fusion partner that presumably stabilizes the whole protein conformation.

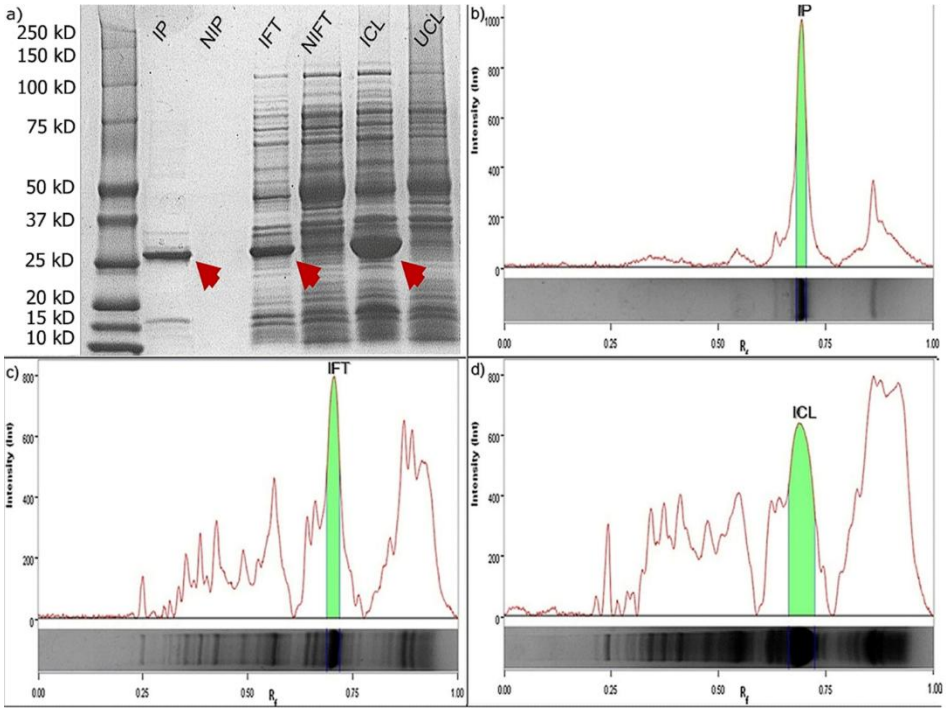

Figure 1. Analysis of SDS-PAGE, a): Coomassie staining of SDS-PAGE showing the six fractions analyzed in the present study. Red arrows show the band corresponding to the protein of interest

according to size. b): Densitometry lane analysis of the IP fraction showing the intensity of the band corresponding to the protein of interest, background subtraction and restriction. c): Densitometry lane analysis of the IFT fraction showing the intensity of the band corresponding to the protein of interest, background subtraction and restriction. d): Densitometry lane analysis of the ICL fraction showing the intensity of the band corresponding to the protein of interest, background subtraction and restriction. Graphs were retrieved from Image Lab 6.1 Software densitometry final report.

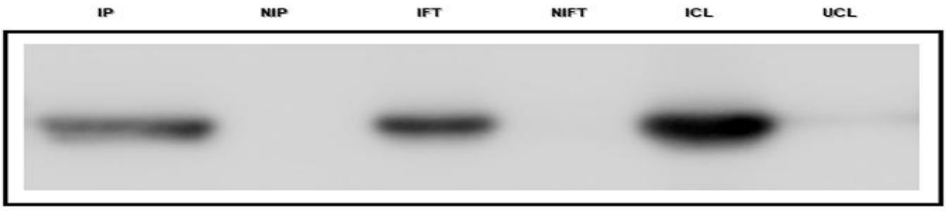

Figure 2. Qualitative Western Blot results showing the band corresponding to the protein of interest in all the IPTG-induced fractions (IP, IFT and ICL) but not in the non-induced ones (NIP, NIFT and UCL).

The present work demonstrates that neither the interaction of the peptide with membranes through the biosynthetic pathway nor its unstructured/unfolded microstates in solution hamper peptide production as a GST-pHLIP fusion protein, being able to produce it at high yields and demonstrating the feasibility of its production as a larger hybrid protein that could be useful for immunization purposes. This is highly relevant to further study of membrane partition pH-responsive peptide synthesis along with offering a production scale-up methodology that could be convenient in certain applications.

Authors' contributions

Study conception and experimental design were done by Oscar Cienfuegos Jiménez, Iván Alberto Marino Martínez and Sergio Bustos Montes. Material preparation and experimental procedures were performed by Oscar Cienfuegos Jiménez, Abril Morales Hernández, Olivia Abigail Robles Rodríguez, Kevin Axel Bañuelos Alduncin, Aurora Rebeca Cortés Castillo, Hugo Daniel Barreto Hurtado and Luis Carrete Salgado. Figure conception and creation were done by Abril Morales Hernández and Kevin Axel Bañuelos Alduncin. Data analysis was performed by Oscar Cienfuegos Jiménez, Iván Alberto Marino Martínez and Abril Morales Hernández. Results discussion was done by Oscar Cienfuegos Jiménez, Iván Alberto Marino Martínez and Olivia Abigail Robles Rodríguez. The manuscript was written by Oscar Cienfuegos Jiménez.

Acknowledgments

We acknowledge the Genomics and Sequencing Unit of the Center for Research and Development in Health Sciences (CIDICS), for kindly providing the Molecular Imager® Gel Doc™ XR System and the ChemiDoc™ XRS+ System.

Conflict of Interest

The authors declare no competing interests.

References

1. Erra Díaz F, Dantas E, Geffner J (2018) Unravelling the Interplay between Extracellular Acidosis and Immune Cells. *Mediators Inflamm* 2018: 1218297. https://doi.org/10.1155/2018/1218297
2. Nguyen VP, Alves DS, Scott HL, et al. (2015) A Novel Soluble Peptide with pH-Responsive Membrane Insertion. *Biochemistry* 54: 6567–6575. https://doi.org/10.1021/acs.biochem.5b00856
3. Weerakkody D, Moshnikova A, Thakur MS, et al. (2013) Family of pH (low) insertion peptides for tumor targeting. *Proc Natl Acad Sci USA* 110: 5834–5839. https://doi.org/10.1073/pnas.1303708110
4. Gupta C, Ren Y, Mertz B (2018) Cooperative Nonbonded Forces Control Membrane Binding of the pH-Low Insertion Peptide pHLIP. *Biophys J* 115: 2403–2412. https://doi.org/10.1016/j.bpj.2018.11.002
5. Scott HL, Westerfield JM, Barrera FN (2017) Determination of the Membrane Translocation pK of the pH-Low Insertion Peptide. *Biophys J* 113: 869–879. https://doi.org/10.1016/j.bpj.2017.06.065
6. Reshetnyak YK, Andreev OA, Segala M, et al. (2008) Energetics of peptide (pHLIP) binding to and folding across a lipid bilayer membrane. *Proc Natl Acad Sci USA* 105: 15340–15345. https://doi.org/10.1073/pnas.0804746105
7. Bauer D, Visca H, Weerakkody A, et al. (2022) PET Imaging of Acidic Tumor Environment With 89Zr-labeled pHLIP Probes. *Front Oncol* 12: 882541. https://doi.org/10.3389/fonc.2022.882541
8. Deskeuvre M, Lan J, Dierge E, et al. (2022) Targeting cancer cells in acidosis with conjugates between the carnitine palmitoyltransferase 1 inhibitor etomoxir and pH (low) insertion peptides. *Int J Pharm* 624: 122041. https://doi.org/10.1016/j.ijpharm.2022.122041
9. Andreev OA, Karabadzhak AG, Weerakkody D, et al. (2010) pH (low) insertion peptide (pHLIP) inserts across a lipid bilayer as a helix and exits by a different path. *Proc Natl Acad Sci USA* 107: 4081–4086. https://doi.org/10.1073/pnas.0914330107
10. Reshetnyak YK, Segala M, Andreev OA, et al. (2007) A monomeric membrane peptide that lives in three worlds: in solution, attached to, and inserted across lipid bilayers. *Biophys J* 93: 2363–2372. https://doi.org/10.1529/biophysj.107.109967
11. Slaybaugh G, Weerakkody D, Engelman DM, et al. (2020) Kinetics of pHLIP peptide insertion into and exit from a membrane. *Proc Natl Acad Sci USA* 117: 12095–12100. https://doi.org/10.1073/pnas.1917857117
12. Adochite RC, Moshnikova A, Carlin SD, et al. (2014) Targeting breast tumors with pH (low) insertion peptides. *Mol Pharm* 11: 2896–2905. https://doi.org/10.1021/mp5002526
13. Sosunov EA, Anyukhovsky EP, Sosunov AA, et al. (2013) pH (low) insertion peptide (pHLIP) targets ischemic myocardium. *Proc Natl Acad Sci USA* 110: 82–86. https://doi.org/10.1073/pnas.1220038110
14. Ding GB, Zhu C, Wang Q, et al. (2022) Molecularly engineered tumor acidity-responsive plant toxin gelonin for safe and efficient cancer therapy. *Bioact Mater* 18: 42–55. https://doi.org/10.1016/j.bioactmat.2022.02.001

15. Stráner P, Taricska N, Szabó M, et al. (2016) Bacterial expression and/or solid phase peptide synthesis of 20-40 amino acid long polypeptides and miniproteins, the case study of Class B GPCR ligands. *Curr Protein Pept Sci* 17: 147–155. https://doi.org/10.2174/1389203716666151102105215
16. Ji T, Lang J, Ning B, et al. (2019) Enhanced Natural Killer Cell Immunotherapy by Rationally Assembling Fc Fragments of Antibodies onto Tumor Membranes. *Adv Mater* 31: e1804395. https://doi.org/10.1002/adma.201804395
17. Trier NH, Hansen PR, Houen G (2012) Production and characterization of peptide antibodies. *Method*s 56: 136–144. https://doi.org/10.1016/j.ymeth.2011.12.001
18. Casey JR, Grinstein S, Orlowski J (2010) Sensors and regulators of intracellular pH. *Nat Rev Mol Cell Biol* 11: 50–61. https://doi.org/10.1038/nrm2820
19. Tsvetkov, P, Myers N, Adler J, et al. (2020) Degradation of Intrinsically Disordered Proteins by the NADH 26S Proteasome. *Biomolecules* 10: 1642. https://doi.org/10.3390/biom10121642
20. Hunt JF, Rath P, Rothschild KJ, et al. (1997) Spontaneous, pH-dependent membrane insertion of a transbilayer alpha-helix. *Biochemistry* 36: 15177–15192. https://doi.org/10.1021/bi970147b
21. Deacon JC, Engelman DM, Barrera FN (2015) Targeting acidity in diseased tissues: mechanism and applications of the membrane-inserting peptide, pHLIP. *Arch Biochem Biophys* 565: 40–48. https://doi.org/10.1016/j.abb.2014.11.002
22. Grimsley GR, Scholtz JM, Pace CN (2009) A summary of the measured pK values of the ionizable groups in folded proteins. *Protein Sci* 18: 247–251. https://doi.org/10.1002/pro.19
23. Spiess M, Junne T, Janoschke M (2019) Membrane Protein Integration and Topogenesis at the ER. *Protein J* 38: 306–316. https://doi.org/10.1007/s10930-019-09827-6
24. Paslawski W, Lillelund OK, Kristensen JV, et al. (2015) Cooperative folding of a polytopic α-helical membrane protein involves a compact N-terminal nucleus and nonnative loops. *Proc Natl Acad Sci USA* 112: 7978–7983. https://doi.org/10.1073/pnas.1424751112
25. Bañó-Polo M, Martínez-Gil L, Barrera FN, et al. (2019) Insertion of Bacteriorhodopsin Helix C Variants into Biological Membranes. *ACS Omega* 5: 556–560. https://doi.org/10.1021/acsomega.9b03126

AIMS Press